

## Summer Soil Moisture Spatiotemporal Variability in Southeastern Arizona

SUSAN STILLMAN,\* JASON NINNEMAN,<sup>+</sup> XUBIN ZENG,\* TRENTON FRANZ,<sup>#</sup> RUSSELL L. SCOTT,<sup>@</sup>  
WILLIAM J. SHUTTLEWORTH,<sup>&</sup> AND KEN CUMMINS\*

\* *Department of Atmospheric Sciences, The University of Arizona, Tucson, Arizona*

<sup>+</sup> *Alaska Satellite Facility, Geophysical Institute, University of Alaska Fairbanks, Fairbanks, Alaska*

<sup>#</sup> *School of Natural Resources, University of Nebraska–Lincoln, Lincoln, Nebraska*

<sup>@</sup> *Southwest Watershed Research Center, Agricultural Research Service, U.S. Department of Agriculture, Tucson, Arizona*

<sup>&</sup> *Department of Hydrology and Water Resources, The University of Arizona, Tucson, Arizona*

(Manuscript received 4 October 2013, in final form 29 April 2014)

### ABSTRACT

Soil moisture is important for many applications, but its measurements are lacking globally and even regionally. The Walnut Gulch Experimental Watershed (WGEW) in southeastern Arizona has measured near-surface 5-cm soil moisture with 19 in situ probes since 2002 within its 150 km<sup>2</sup> area. Using various criteria to identify erroneous data, it is found that in any given period from 1 July to 30 September from 2002 to 2011, 13–17 of these probes were producing reasonable data, and this is sufficient to estimate area-averaged seasonal soil moisture. A soil water balance model is then developed using rainfall as its only input to spatially extrapolate soil moisture estimates to the 88 rain gauges located within the watershed and to extend the measurement period to 56 years. The model is calibrated from 2002 to 2011 so that the daily in situ and modeled soil moisture time series have a high average correlation of 0.89 and a root-mean-square deviation of 0.032 m<sup>3</sup> m<sup>-3</sup>. By interpolating modeled soil moisture from the 88 rain gauges to a 100-m gridded domain over WGEW, it is found that spatial variability often increases when 88 (rather than 13–17) estimates are taken. While no trend in the spatial average surface soil moisture is found, large variability in the spatial average soil moisture from 1 July to 30 September is observed from year to year, ranging from 0.05 to 0.09 m<sup>3</sup> m<sup>-3</sup>. In addition to spatiotemporal analysis of WGEW, this gridded soil moisture product from 1956 to 2011 can be used for validation of satellite-based and reanalysis products and land surface models.

### 1. Introduction

Soil moisture has impacts in many fields, such as meteorology, climatology, hydrology, agriculture, and water management. Soil moisture “memory”—the slow response to changes in precipitation input—is an important climate driver and is a critical variable in predicting rainfall, particularly over the midlatitudes (Eltahir 1998; Koster and Suarez 2001; Seneviratne et al. 2006). Orth et al. (2013) found that a simple water balance model based on precipitation, net radiation, and streamflow observations can be used to simulate soil moisture memory and seasonal anomalies. Anomalies in soil moisture have also been shown to affect the North American monsoon system (Small 2001). Root-zone moisture affects plant

health, and good watershed management depends on knowing and predicting soil moisture dynamics, particularly in drier regions (Vereecken et al. 2008).

Soil moisture is generally undersampled because of its spatial heterogeneity. For instance, Zreda et al. (2012) showed that within a circular area with a diameter of approximately 400 m in the San Pedro River valley of southeastern Arizona, individual instantaneous 0–5-cm depth soil moisture measurements range from 0.06 to 0.37 m<sup>3</sup> m<sup>-3</sup> and that over 10 profiles are needed within the 400 m diameter to estimate average soil moisture within 0.03 m<sup>3</sup> m<sup>-3</sup>. However, because of its temporal stability, fewer measurements are required to capture the temporal variability of soil moisture. For example, Brocca et al. (2012) showed that the spatial correlation of soil moisture measurements at multiple locations on one day versus measurements at the same locations separated by several weeks is significant.

While satellite retrievals are useful to obtain information on continental-scale near-surface soil moisture,

Corresponding author address: Susan Stillman, The University of Arizona, Physics–Atmospheric Sciences Bldg., Rm. 542, 1118 E. 4th St., P.O. Box 210081, Tucson, AZ 85721-0081.  
E-mail: sstill88@email.arizona.edu

the spatial and temporal resolution is too coarse to gain insight on watershed-scale hydrologic processes (Crow et al. 2012). Ryu et al. (2010) showed that intermediate-scale factors in soil moisture dynamics such as vegetation and high rock fraction significantly skew satellite-retrieved soil moisture, but that improvements to soil moisture can be made using a rock fraction correction. Validating satellite-based soil moisture retrievals from ground-based measurements is subject to complications associated with upscaling point measurements to a coarse grid (Crow et al. 2012). To bridge this gap, aircraft measurements during the Southern Great Plains 1997 (SGP97) Hydrology Experiment and Soil Moisture Experiment 2004 (SMEX04) in southeastern Arizona retrieved soil moisture at a spatial and temporal scale in between satellite and point source measurements during satellite overpasses. Jackson et al. (1999) found that it is possible to extrapolate soil moisture retrieval algorithms from surface observations to satellite measurements based on a comparison of in situ measurements with the aircraft-borne Electronically Steered Thinned Aperture Radiometer (ESTAR)-retrieved product with a spatial scale (800 m) useful for upscaling to projected satellite footprints (~10 km).

Over the Walnut Gulch Experimental Watershed (WGEW) of about 150 km<sup>2</sup>, also in the San Pedro River valley of southeastern Arizona, there are 19 soil moisture probes and 88 rain gauges from which soil moisture can be inferred, giving it an average measurement density of one in situ soil moisture sample per 7.9 km<sup>2</sup> or one modeled soil moisture estimate per 2 km<sup>2</sup>. These densities are more than two orders of magnitude finer than that (one sample per ~1760 km<sup>2</sup>) in the Oklahoma Mesonet, which represents one of the best networks for mesoscale meteorological measurements ([www.mesonet.org](http://www.mesonet.org)).

One purpose of this study is to develop a long-term summer soil moisture dataset over WGEW that can be used to characterize the spatiotemporal variability of soil moisture and to evaluate other soil moisture products [e.g., from remote sensing retrievals such as the Soil Moisture Ocean Salinity mission (Kerr et al. 2001)] and, when available, the Soil Moisture Active Passive mission (Entekhabi et al. 2010) and land surface data assimilation (Xia et al. 2012). Such a dataset can also be used to infer initial surface soil moisture conditions for surface runoff models.

Land surface models require many inputs, which are not always readily available. Models that use only precipitation as input are limited in capability, but in the absence of other meteorological data, they are often the best option for soil moisture estimation. An antecedent precipitation index (API) is sometimes

used to estimate soil moisture from a weighted sum of the precipitation over a preceding period. Pan et al. (2003) used a method similar to API to estimate summer soil moisture directly from dynamic soil moisture equations without requiring initial soil moisture conditions. Pan (2012) expanded on this model so that it is appropriate for year-round use by estimating the annual cycle of the loss coefficient (related to evapotranspiration). Pellarin et al. (2013) also estimated soil moisture from an API-based model to adjust satellite precipitation estimates by comparing the brightness temperature from satellite soil moisture retrievals to modeled brightness temperatures from this API-modeled soil moisture.

Over WGEW, a water balance approach was used to estimate soil moisture in a case study by Rim and Gay (2002). While their results have physical implications for the various terms in a basic surface energy balance, their method requires both flux measurements and runoff data, and the areal coverage is limited to a few point measurements over the period from 17 July to 15 August 1990. Houser et al. (1998) tested various data assimilation techniques to assimilate aircraft measurements with a TOPMODEL-based (Beven and Kirkby 1979) land model over WGEW. Compared with in situ measurements during the Monsoon '90 Multidisciplinary Large Scale Field Experiment (Kustas and Goodrich 1994), they found that a simple statistical correction algorithm performs almost as well over WGEW as more complicated methods and with relatively low computational time. Das et al. (2008) assimilated aircraft measurements with a more complicated land model over WGEW during SMEX04 to observe the time evolution of soil moisture profiles and emphasized the benefits of incorporating soil layer information in the model. Compared with these studies, we use a water balance model forced by rain gauge precipitation data only and calibrated by collocated soil moisture measurements to infer hourly near-surface (~5 cm) soil moisture for 56 years over WGEW.

Specifically, this study will address three questions. How well does the in situ network measure summer soil moisture in WGEW? Is it possible to estimate summer soil moisture from precipitation measurements only so that we can extend the data period from 10 years of in situ measurements to 56 years of modeled soil moisture and increase the spatial density of measurements from 19 soil moisture measurement sites to 88 rain gauge sites? What are the temporal and spatial variability of summer (from 1 July to 30 September) soil moisture over WGEW? Section 2 describes the datasets and our analysis methods, section 3 presents the results, and section 4 gives the conclusions.

## 2. Methods and datasets

### a. Location and instruments

The WGEW is an approximately 150 km<sup>2</sup> area surrounding Tombstone, located in southern Arizona, and is a subwatershed of the larger San Pedro watershed. It is a semiarid region with an average of 350 mm annual precipitation, about 60% of this occurring during the months of July–September (Stillman et al. 2013). The northeast corner of the watershed borders the Dragoon Mountains, and the Tombstone hills lie to the west. The watershed is dominated by sandy, gravelly loams with small-scale landforms that have slopes ranging from moderate to steep (Osterkamp 2008). The main vegetation types are grassland and shrub. In a multiple-day survey during SMEX04, approximately 40 sites were sampled for rock fraction, revealing a median rock fraction of 15.19% by volume, with values ranging from 0.97% to 43.88% (Jackson and McKee 2009). The town of Tombstone is located within the watershed with an area of 11 km<sup>2</sup>, of which only a small stretch (~2 km<sup>2</sup>) along the main highway is urbanized. A detailed description of the geology, topography, hydrology, vegetation, and climatology of WGEW is given by USDA (2007).

The U.S. Department of Agriculture–Agricultural Research Service (USDA-ARS) maintains a suite of instruments throughout WGEW, including 88 rain gauges and 19 Stevens Hydra Capacitance Probes collocated with rain gauges (Goodrich et al. 2008; Keefer et al. 2008), which measure soil moisture at a depth of ~5 cm as a function of dielectric properties of the soil with temperature adjustments. The gauge network collects 1-min resolution precipitation data and has been in place since 1956, while the soil moisture probe network collects 30-min data and has been in use since 2002. The locations of the current 88 gauges and 19 soil moisture probes are shown in Fig. 1.

The most accurate way of determining soil moisture is to sample and measure the soil water content directly using gravimetric techniques. This “ground truth” soil moisture is found by the mass difference of the sample before and after heating it to evaporate the water. However, this method is not practical for long-term measurements, so indirect methods must be used to measure soil moisture. Electrical sensors (such as the Stevens Hydra Probes) provide an indirect method of estimating volumetric soil moisture by measuring the capacitance and conductivity properties of the soil while correcting for temperature effects. For these sensors, the measurement volume around the probe is small. Air gaps, roots, and varying levels of probe contact with the soil can have a large effect on the output data. They are also

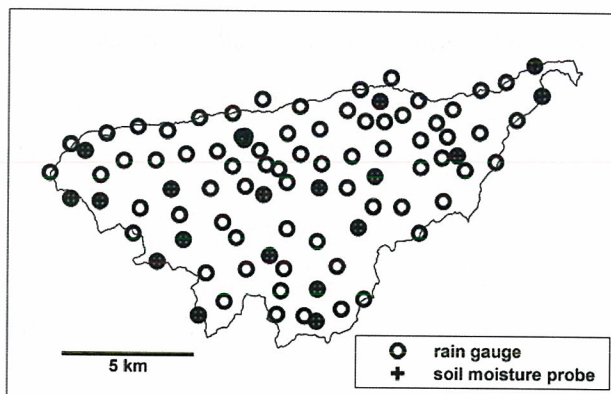


FIG. 1. Locations of 88 rain gauges and 19 soil moisture probes over WGEW centered at 31°43'N, 110°41'W.

very sensitive to direct contact with water. For example, a water-filled cavity in the soil or an exposed probe tine results in unrealistic spikes in the inferred soil moisture. Robinson et al. (2008) provided a description of challenges related to estimating soil permittivity, which is used in the estimation of soil moisture in capacitance probes.

In this study, the 1-min rainfall data for the 88 rain gauges in WGEW (available at [www.tucson.ars.ag.gov/dap/](http://www.tucson.ars.ag.gov/dap/)) are converted to 30-min rainfall to be consistent with the soil moisture measurements. Soil moisture data from in situ probes are quality controlled: data are not used for model calibration when the data are missing or are determined to be of poor quality (section 3). We focus on the observations from 1 July to 30 September, because these months encompass most of the summer rainy season or monsoon in southern Arizona and are responsible for the majority of the annual precipitation. Soil moisture data for 10 years (from 2002 to 2011) and rain gauge data for 56 years (from 1956 to 2011) are used here.

### b. Water balance model

In general, to drive a land surface model to compute soil moisture, temperature, and often surface energy and water fluxes, comprehensive near-surface measurements of precipitation, downward solar and longwave radiative fluxes, air temperature, humidity, and wind are needed (e.g., Dai et al. 2003). Such measurements are usually available from flux towers only. However, recent work has shown that good soil moisture simulations can be found using hourly precipitation and temperature data only optimized with weekly in situ measurements (Brocca et al. 2013) and using daily precipitation and solar radiation data optimized with daily streamflow (Orth et al. 2013). To make use of the precipitation data from the 88 rain gauges in WGEW, here we estimate volumetric

soil moisture based on a water balance model forced by precipitation only using the following equations:

$$\theta_t = \theta_{t-1} + \frac{\Delta T}{Z} \left\{ (1 - B^4) [\min(p_t - I, p_{\text{crit}})] - EA^\beta - a_1 A^{a_2} \right\}, \quad (1)$$

$$A = \frac{\theta_{t-1} - \theta_w}{\theta_{\text{th}} - \theta_w} \quad \text{for } 0 \leq A \leq 1, \quad (2)$$

$$B = \frac{\theta_{t-1}}{\theta_s} \quad \text{for } 0 \leq B \leq 1, \quad \text{and} \quad (3)$$

$$I = \min(I_m, p_t), \quad (4)$$

where  $I$  is the intercepted precipitation, with  $I_m$  being the maximum amount of precipitation that can be intercepted by canopy ( $\text{mm h}^{-1}$ );  $Z$  is the layer depth (mm);  $\Delta T$  is the time step (h);  $\theta_t$  and  $\theta_{t-1}$  are volumetric soil moistures ( $\text{m}^3 \text{m}^{-3}$ ) at time  $t$  and  $(t - \Delta T)$  constrained between  $\theta_w$  and  $\theta_s$  (effective minimum and saturated soil moisture values);  $\theta_{\text{th}}$  is the threshold soil moisture ( $\text{m}^3 \text{m}^{-3}$ ) over which the evaporation rate is assumed constant;  $p_t$  is precipitation rate, with  $p_{\text{crit}}$  being the precipitation rate ( $\text{mm h}^{-1}$ ) above which all precipitation becomes direct runoff; and  $a_1$  ( $\text{mm h}^{-1}$ ),  $a_2$  (unitless), and  $\beta$  (unitless) are calibrated constants greater than zero.

The surface evapotranspiration term  $E$  is the sum of potential surface evaporation and the small portion of transpiration that comes from the surface soil layer ( $\text{mm h}^{-1}$ ). It is a function of net radiative flux and hence has a pronounced diurnal cycle. The evapotranspiration data are available for limited periods from the Bowen ratio measurements at the Kendall site within WGEW (also available at [www.tucson.ars.ag.gov/dap/](http://www.tucson.ars.ag.gov/dap/)), and their averaged diurnal cycle from 1 July to 30 September for all years with measurements available (1997–2007; Fig. 2) is used to estimate  $E$ . However, the measured evapotranspiration includes  $E$  and transpiration from the vegetation root zone. Therefore, we take the diurnal maximum value  $E_{\text{max}}$  as a calibrated parameter, which should be less than that from measured evapotranspiration. Furthermore, we take the diurnal minimum value  $E_{\text{min}}$  simply as  $0.1E_{\text{max}}$  in Fig. 2 to be consistent with the  $E_{\text{min}}-E_{\text{max}}$  ratio from the Kendall flux measurements. The diurnal cycle of  $E$  in Fig. 2 is then applied in the model.

Physically, the first term in the bracket of Eq. (1) represents the fraction of rainfall that reaches the surface and infiltrates downward. Rainfall intercepted by plants (i.e.,  $I$ ;  $\text{mm h}^{-1}$ ), is related to the vegetation fraction and leaf area index, but here it is simply computed from Eq. (4). The factor  $B^4$  in the runoff term  $\min(p_t - I, p_{\text{crit}})B^4$  is based on the Biosphere–Atmosphere Transfer Scheme

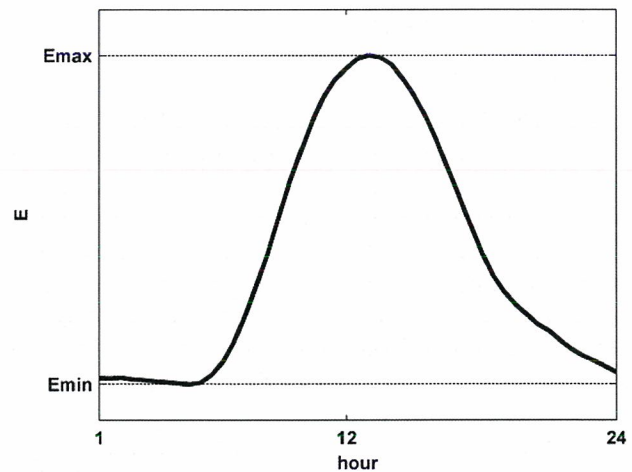


FIG. 2. The diurnal cycle of max surface evapotranspiration  $E$  ( $\text{mm h}^{-1}$ ) in Eq. (1) as a function of local hour, as estimated from flux measurements at the Kendall site in WGEW. The variable  $E_{\text{min}}$  is approximately  $1/10$  of  $E_{\text{max}}$ , and  $E_{\text{max}}$  is provided in Table 1.

(Dickinson et al. 1993). The second term (surface evapotranspiration)  $EA^\beta$  is adapted from the Noah land surface model (Ek et al. 2003). For simplicity, capillary movement is ignored, and the Green–Ampt equation (Green and Ampt 1911) for vertical soil water flux is simplified so that drainage rate simply equals the soil conductivity. Van Genuchten (1980) defined relative soil conductivity as a function of  $A$  in Eq. (2), which is approximately exponential. Therefore, we define the downward soil moisture flux (infiltration; term 3) as a calibrated exponential function of water content, represented by the last term in Eq. (1).

Table 1 shows values for all the parameters in Eq. (1). For  $E_{\text{max}}$  of  $0.34 \text{ mm h}^{-1}$  in Table 1,  $E_{\text{min}}$  is simply taken as  $0.1E_{\text{max}}$  in Fig. 2, or  $0.034 \text{ mm h}^{-1}$ . The minimum soil moisture (i.e.,  $\theta_w$ ) varies with location, and its determination will be discussed in section 3b. Some model parameters are chosen based on physical measurement considerations, such as  $Z$ , which is chosen to surround the 5-cm depth probe, and  $\Delta T$ , which is chosen to be consistent with the probe time step. To assign values to the remaining model parameters, the coefficients are adjusted within a plausible range, and the optimal set of coefficients is selected based on a variety of considerations. For each variable, seven values spaced evenly in parameter space are selected to span the plausible range, and every combination of these values is tested in the model against in situ soil moisture using precipitation at its collocated gauge. The “best” parameter set would ideally result in the average of all in situ soil moisture and the average of all collocated modeled soil moisture having the lowest root-mean-square deviation (RMSD) and highest correlation.

TABLE 1. Soil moisture model parameter values.

Parameter	Value
$\Delta T$	0.5 h
$E_{\max}$	0.34 mm h <sup>-1</sup>
$I_m$	0.3 mm h <sup>-1</sup>
$p_{\text{crit}}$	40 mm h <sup>-1</sup>
$\theta_s$	0.35 m <sup>3</sup> m <sup>-3</sup>
$\theta_{\text{th}}$	0.28 m <sup>3</sup> m <sup>-3</sup>
$\beta$	1.4
$a_1$	0.3 mm h <sup>-1</sup>
$a_2$	2
$Z$	75 mm

However, there is not a parameter set within the plausible range that fits both criteria. While it is possible to find multiple unphysical parameter sets that will create low RMSD values, requiring high correlation values ensures that certain dynamics, such as the dry down curve after rain events, are well fit. Therefore, the likelihood of the parameters having physical meaning is high. In performing this parameter search, the best correlation and RMSD parameters lie along the parameter value extremes, which brings into question the physical realness of these results. Therefore, a visual analysis is done by sorting all parameter sets in order from highest to lowest RMSD and lowest to highest correlation and identifying if each parameter converges onto a single value. When this is done for the all-gauge average, there is no convergence that does not occur along the parameter extremes, so this is done for each probe location separately. The parameters used in the model are the average of the parameters at each probe where there is convergence.

Cosh et al. (2008) noted that, due in part to unstable sensors, the rainfall response of soil moisture is not linearly related to in situ probes. Therefore, only the high-quality soil moisture data (see further discussion in section 3a) are used. Second, the summer runoff–rainfall ratio within WGEW, depending on the spatial scale, should be in the vicinity of ~5%–20% as suggested by Goodrich et al. (2008), the surface evapotranspiration term should be lower than the total evapotranspiration from flux tower measurements, and precipitation interception should be relatively small (e.g., less than 10%) over semiarid regions with limited vegetation cover. Therefore, any set of parameters that produces a maximum runoff–rainfall ratio for all summers greater than 0.25 or interception–rainfall ratio greater than 0.15 is thrown out. The robustness of this technique is tested by looking at the parameter values found in each year separately versus the all-year parameter values for each gauge, and generally the results are similar, although the best RMSD and correlation values vary from year to year. It is important to note that because the calibration is

done in WGEW during the summer months, this specific set of model parameters is appropriate only for the summer months in WGEW. For other regions or periods of the year, while the above model may still be useful, the parameters may differ significantly.

Using Eq. (1) with coefficients in Table 1, 30-min soil moisture data are generated over each gauge site in WGEW for the whole 56 years. Recognizing the simplifications in Eq. (1) (e.g., the fixed diurnal cycle of  $E$  in Fig. 2), it may be more reasonable to use daily mean soil moisture, so the 30-min estimated and observed soil moisture are converted to daily for comparison. As precipitation has a strong diurnal cycle over WGEW (Stillman et al. 2013) and soil moisture depends on both precipitation amount and intensity, it is beneficial to run the model in half-hourly (rather than daily) time steps. We also found some spurious diurnal variations in the 30-min measurements similar to the diurnal variations by the dielectric-based soil moisture sensors that Verhoef et al. (2006) attributed to sensor sensitivity to temperature effects. Hence, the daily mean measurements are also more reasonable (than 30-min values), and therefore, daily values are used for model evaluation and data analysis in the next section.

### 3. Results and discussion

#### a. In situ soil moisture data quality

Probes that infer soil moisture from electric properties of the soil such as time domain reflectometry and capacitance probes are often used because of their ability to continuously measure soil moisture. With 19 capacitance probes spanning the 150 km<sup>2</sup> area, the WGEW has one of the densest in situ measurement networks over a large watershed. This large set of observations with collocated gauge data makes measurement errors apparent from visual inspection. Although certain quality control measures (i.e., visual inspection, removal of data from station not in operation, computer failure, etc.) described by Keefer et al. (2008) were done by USDA-ARS, to replace existing false values with missing values, we included further criteria to remove data that most likely contains large errors. The criteria we used to determine “bad” data are zero values for soil moisture (e.g., Fig. 3b), data being nonresponsive to significant rain events, continuous soil moisture values significantly greater than the assumed saturation value ( $\theta_s = 0.35 \text{ m}^3 \text{ m}^{-3}$ ; e.g., due to water pockets surrounding the probe from surface erosion with time), and very large diurnal variability. Very large diurnal variability could indicate sensor error or the probe being at a shallower depth, which can occur through surface erosion. To be

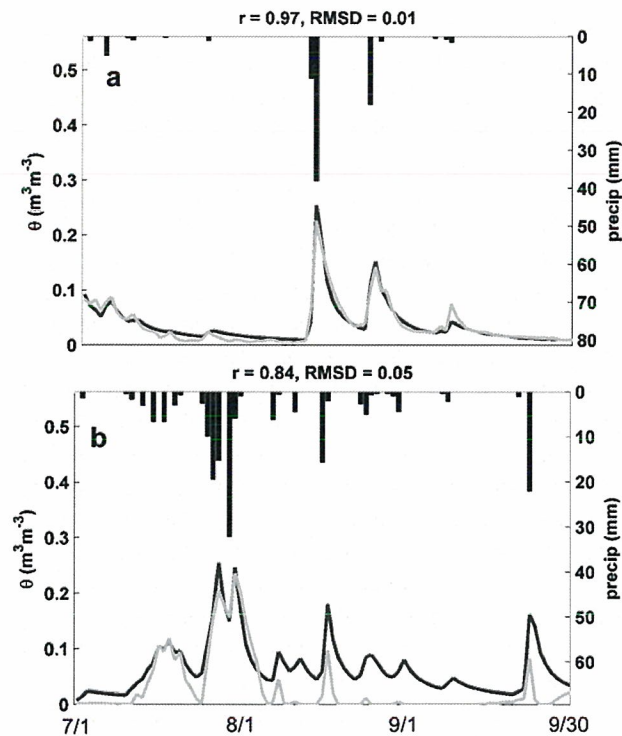


FIG. 3. Daily precipitation (bars), in situ soil moisture (gray), and modeled soil moisture at a collocated gauge (black) for a (a) “good” fit (gauge 100; 2009) and (b) “poor” fit (gauge 34; 2010) from 1 Jul to 30 Sep. Correlation and RMSD of modeled to in situ soil moisture are labeled.

sure that our model is being calibrated only with probes at a consistent 5-cm depth, these probes should not be included. For zero-rain days, the possible diurnal range of soil moisture can be estimated from Eq. (1). From these calculations and based on our experience, we set the maximum diurnal range of soil moisture for zero-rain days as  $0.06 \text{ m}^3 \text{ m}^{-3}$ . Any probe with more than 5% of its diurnal ranges on zero-rain days greater than this value in any year is considered “bad” for that year.

While the soil moisture probes are assumed to have higher accuracy in their measurement than the water balance model in Eq. (1), problems arise regarding what they are actually measuring. For example, a pocket of water surrounding the probe can cause an unrealistic spike in the soil moisture value. This is seen in some of the half-hourly soil moisture time series. Another shortcoming of the probes is that through surface erosion, the probe depth changes over time, which can affect the time scale and magnitude to which the soil responds to precipitation input. This may be the case in Fig. 3b because, compared with the model, the characteristics that the measured soil moisture exhibits (i.e., quicker drying than expected and drying to zero after rain events) would likely be closer to the surface. The probes themselves are also subject to accuracy loss or drift over time.

TABLE 2. No. of situ soil moisture capacitance probes with data and with obvious error for each year.

	No. available	No. determined to be of poor quality
2002	18	2
2003	17	2
2004	17	2
2005	15	1
2006	16	3
2007	17	1
2008	17	1
2009	17	1
2010	19	2
2011	15	1

Table 2 shows the number of probes with data available for the entire period from 1 July to 30 September for each year and the number of probes with obvious error. The actual number of good available gauges in each year ranges from 13 to 17, and these are the data used in our work, as mentioned in section 2b.

#### b. Model evaluation

Whereas Peters-Lidard et al. (2008) estimated soil moisture using entirely independent soil texture parameters for eight sites within WGEW, we are considering a large number of sites and interpolating data to the entire watershed. Therefore, we use a single set that best fits the population of in situ measurements, with the exception of allowing the effective minimum soil moisture (i.e.,  $\theta_w$ ) to vary from site to site. The site-specific  $\theta_w$  is estimated by the measured soil moisture after a long period of no precipitation. Because there is generally from little to no precipitation in May and early June (well before the arrival of the North American monsoon), we first compute the minimum of daily mean soil moisture in June at each soil moisture probe each year. To account for wetter-than-average Junes, any year during which soil moisture values do not drop below  $0.1 \text{ m}^3 \text{ m}^{-3}$  is ignored. The median of these minimum values for all years at each probe is taken as  $\theta_w$  for that location. These  $\theta_w$  values are then interpolated using the two-dimensional second-order inverse distance weighting scheme of Garcia et al. (2008) to all rain gauge locations for which in situ  $\theta_w$  is unavailable.

To use Eq. (1) to infer soil moisture, an initial condition of soil moisture is needed for each summer. Because there can be rainfall events before the 1 July start, the initial soil moisture conditions from 1 July to 30 September vary from year to year at each location. Because observed soil moisture data are not available prior to 2002 over WGEW (except during field experiments), we cannot take 1 July as the initial time. Instead, the model is run starting on 1 June for each year,

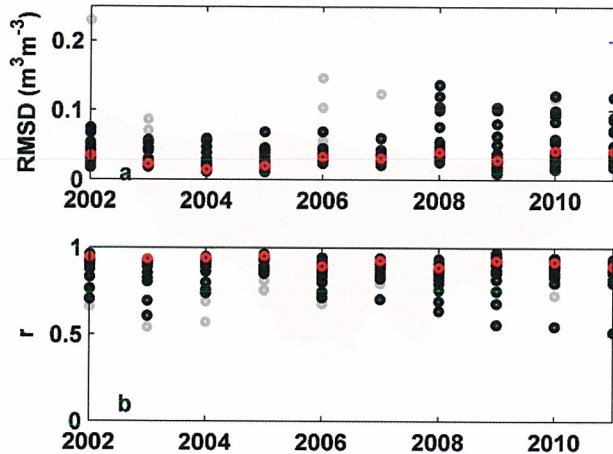


FIG. 4. (a) RMSD between daily in situ and modeled soil moisture at each collocated rain gauge for the period from 1 Jul to 30 Sep in each year and (b) correlation between daily in situ and modeled soil moisture for all available probes (all circles), probes without obvious measurement error (black), and for the avg of all in situ probes vs all modeled soil moisture from collocated gauges (red).

assuming an initial soil moisture value of  $\theta_w$ . There is generally little to no precipitation leading up to 1 June so this assumption is reasonable. This study only uses soil moisture values between 1 July and 30 September of each year for analysis. The values for  $\theta_w$  range from 0.0001 to  $0.03 \text{ m}^3 \text{ m}^{-3}$ .

To evaluate the water balance model in Eq. (1), the computed soil moisture time series are compared with measurements at the 19 stations with in situ probes collocated with rain gauges. Figure 3 shows two of these comparisons: Fig. 3a shows a relatively good fit and Fig. 3b shows one of the poorest fits, with correlation values of 0.97 and 0.84 and RMSD of  $0.0093$  and  $0.047 \text{ m}^3 \text{ m}^{-3}$ , respectively. These two examples illustrate how well the model performs in certain scenarios and how poorly the fit with observations can be due to either model or probe error.

Figure 4 shows the RMSD and correlation between daily modeled and measured soil moisture values. In general, the soil moisture estimates agree better with measurements when only probes without obvious errors are used (black circles). Even when all probes for all periods with continuously available data are used, the median RMSD of all modeled daily soil moisture time series with its collocated in situ time series is just  $0.034 \text{ m}^3 \text{ m}^{-3}$  and the median correlation is 0.889 (statistically significant at  $<0.001$  level), which is similar to the median values found using only “good” sites ( $0.032 \text{ m}^3 \text{ m}^{-3}$  and 0.891). The difference is more apparent in comparing the poorest fits; 75% of the daily time series for the “good” sites have an RMSD less than  $0.048 \text{ m}^3 \text{ m}^{-3}$  and correlation greater than 0.84

(significant at  $<0.001$  level) compared with 0.053 and 0.83 for all sites (Fig. 4). There is also a large difference in the correlation of the poorest fit 30-min data when the “bad” gauges are removed. While the in situ probes on average estimate wetter annual soil moisture than the model, the soil moisture dynamics are captured very well by the model, with average temporal standard deviations (from daily all-gauge averages) of  $0.041$  and  $0.042 \text{ m}^3 \text{ m}^{-3}$  for the modeled and in situ averages, respectively.

Assessing location-specific parameters for each gauge is difficult, so some generalizations have been made, which in some cases can limit the accuracy of the model. Different soil properties from site to site cause some of the parameters, including the maximum surface evapotranspiration rate (i.e.,  $E_{\text{max}}$ ) and the precipitation threshold (i.e.,  $p_{\text{crit}}$ ) to vary. This could also contribute to uncertainties in model results in Figs. 3 and 4. Note that some of the differences between estimated and observed soil moisture values in Figs. 3 and 4 are probably caused by measurement uncertainties. For instance, for the poor case in Fig. 3, the measured soil moisture does not respond to some of the small precipitation events. The measurements also show the unlikely soil moisture values of  $0 \text{ m}^3 \text{ m}^{-3}$ . As mentioned earlier, such measurements (with zero soil moisture) are not used in the calibration of the model.

### c. Data analysis

To assess the spatial distribution of soil moisture, we interpolate estimated soil moisture over all gauge sites to fine grid cells of  $100 \text{ m} \times 100 \text{ m}$  over WGEW based on the two-dimensional second-order inverse distance weighting scheme of Garcia et al. (2008). This simple interpolation method has been used operationally for a long time over WGEW. Its validity is determined here using soil moisture estimated over all gauge sites. For each year, one gauge is “removed” at a time and the daily soil moisture data at all other gauges are interpolated to that location. The interpolated values are then compared with the original values at this location. The average correlation is 0.95 and RMSD is  $0.015 \text{ m}^3 \text{ m}^{-3}$ , demonstrating that, indeed, this method works well for soil moisture interpolation over WGEW.

The best interpolation grid depends on the purpose of the study. For comparison with other datasets (e.g., from satellites and aircraft), it is appropriate to choose a comparable grid size. If one wants to ignore microscale features, too fine of a grid size is not appropriate. In this study, the grid size is chosen so that the final product has a set of statistics that mimics the gauge statistics. In this way, we can visualize the distribution of soil moisture while keeping the results to the truest available values: the soil moisture estimated at each rain gauge. Using a

larger grid causes a loss of spatial variability and the choice of a 100-m grid allows us to approximately maintain the spatial variability observed using gauges.

To illustrate the difference between the 100-m grid and coarser grid resolutions, we computed the spatial range (highest minus lowest soil moisture at any grid box on a given day) of daily mean soil moisture for each day using all gauges, 100-m grids, and 1000-m grids from 1956 to 2011. Then, we compute the histogram of the differences of results using 100-m grids versus using all gauges. The 50th (i.e., median), 75th, and 90th percentiles are found to be 0.020, 0.033, and  $0.048 \text{ m}^3 \text{ m}^{-3}$ , respectively. These values become larger ( $0.033$ ,  $0.064$ , and  $0.095 \text{ m}^3 \text{ m}^{-3}$ ) for the differences between 1000-m grids and all gauges. It is also noted that the difference between the soil moisture at each of the gauges and the grid box encompassing it decreases with the smaller grid, and using the 100-m grid has an RMSD less than  $0.01 \text{ m}^3 \text{ m}^{-3}$ . On average, the spatial standard deviation and coefficient of variation (CV; defined as the standard deviation normalized by the mean) of the daily 100- and 1000-m interpolated soil moisture are nearly the same; however, the spatial range is much larger ( $0.066 \text{ m}^3 \text{ m}^{-3}$ ) for the 100-m grid than for the 1000-m grid ( $0.034 \text{ m}^3 \text{ m}^{-3}$ ). Note that the model does not account for the urbanized area of Tombstone that would be resolved under a 100-m grid, but the urbanized area is too small ( $\sim 2 \text{ km}^2$ ) to affect most comparable products over WGEW of  $\sim 150 \text{ km}^2$ .

Figure 5 shows the spatial pattern (100-m grid) of daily averaged soil moisture before, during, and after a sequence of rainfall events. On 2 September 1975 (before any precipitation events), there is relatively low spatial variability in soil moisture. Following precipitation events on 3–5 September (with a total rainfall amount of 20.9 mm), there is much higher variability with a spatial soil moisture range of  $0.18 \text{ m}^3 \text{ m}^{-3}$  across the watershed on 5 September. With additional rainfall on 6–8 September (with a total amount of 19.5 mm), the watershed becomes wetter, and the spatial range of soil moisture becomes smaller ( $0.13 \text{ m}^3 \text{ m}^{-3}$ ) on 8 September (compared with that on 5 September). The spatial standard deviation on 5 and 8 September are 0.020 and  $0.017 \text{ m}^3 \text{ m}^{-3}$ , respectively. This event is representative of the soil moisture response to a typical localized precipitation event and demonstrates the high degree of spatial variability that can be observed in daily soil moisture within the watershed.

Figure 6 summarizes the spatial and temporal variations in daily mean soil moisture for two years [dry, 1960 (100.1 mm total summer rain); wet, 1999 (326.9 mm total summer rain)], and a comparable degree of variability is apparent among all years. The interquartile range (i.e.,

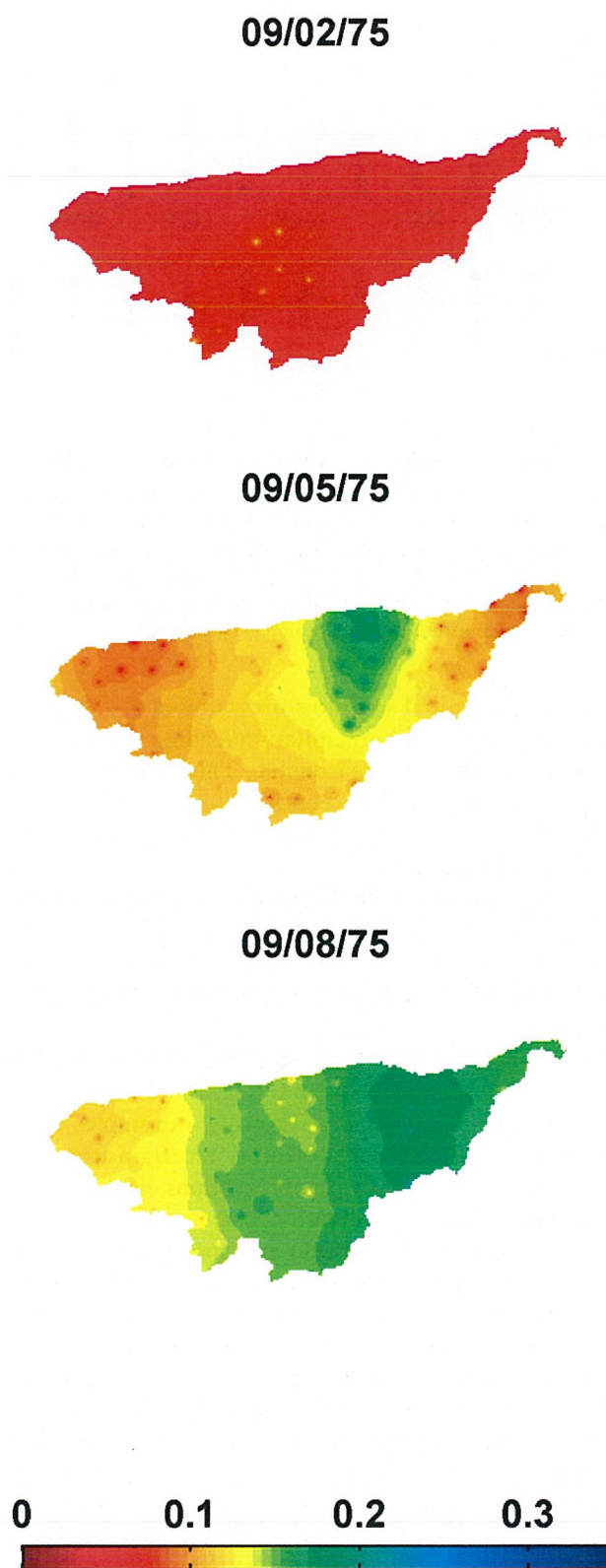


FIG. 5. Spatial distribution of daily avg soil moisture ( $\text{m}^3 \text{ m}^{-3}$ ) for 2, 5, and 8 Sep 1975 over WGEW centered at  $31^{\circ}43' \text{N}$ ,  $110^{\circ}41' \text{W}$ .

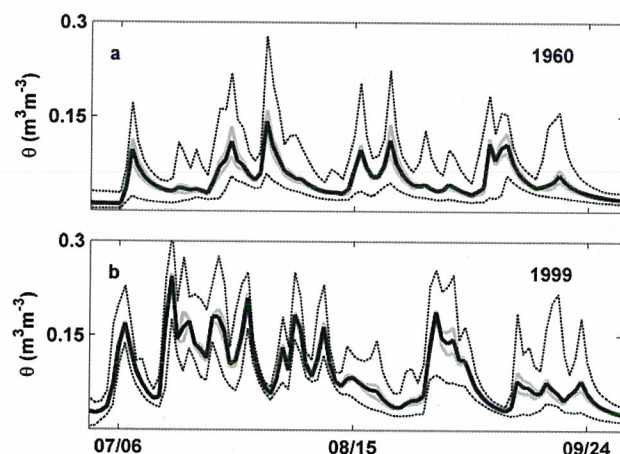


FIG. 6. Spatially averaged (over all  $100\text{ m} \times 100\text{ m}$  grid cells) daily soil moisture (solid black), 25th and 75th percentile soil moisture values (gray), and min and max soil moisture values (dotted black) within WGEW for (a) 1960 and (b) 1999.

the difference between 25th and 75th percentiles) of soil moisture in Fig. 6a peaks at  $0.048\text{ m}^3\text{ m}^{-3}$  and is highest after precipitation events, where the average soil moisture increases. The two years are chosen to examine spatial characteristics of soil moisture under different annual precipitation conditions: 1960 (Fig. 6a) is a relatively dry year, whereas 1999 (Fig. 6b) is a relatively wet year (Stillman et al. 2013). The temporal average of spatial range is  $0.079\text{ m}^3\text{ m}^{-3}$  in both the dry and wet years. The maximum spatial range of daily mean soil moisture is as high as  $0.27\text{ m}^3\text{ m}^{-3}$  during the entire time period of this study, which is near the maximum possible range ( $\theta_s - \theta_w$ ).

Figures 5 and 6 also show a large temporal variability of spatially averaged daily mean soil moisture within a season. Within 6 days, the spatially averaged soil moisture increases from  $0.06\text{ m}^3\text{ m}^{-3}$  on 2 September to  $0.15\text{ m}^3\text{ m}^{-3}$  on 8 September 1975 (Fig. 5). For a dry year (Fig. 6a), the spatially averaged soil moisture varies from  $0.01$  to  $0.15\text{ m}^3\text{ m}^{-3}$ , while it varies from  $0.03$  to  $0.24\text{ m}^3\text{ m}^{-3}$  in a wet year (Fig. 6b).

Table 3 shows the average spatial and temporal ranges, standard deviations, and coefficients of variation for modeled soil moisture at all rain gauges, all gauges that are collocated with in situ soil moisture probes, and in situ soil moisture probes for the 10 years that in situ measurements are available. The temporal statistics are based on the average from daily spatially averaged soil moisture, and the spatial statistics are based on the average of all daily averaged soil moisture at all gauges. Comparing the all-gauge and in situ statistics, it is clear that the model follows the average temporal quantities of the in situ probes closer than the spatial quantities. These results lead us to believe that while the model

TABLE 3. Avg spatial (sp) and temporal (tm) ranges (=max – min;  $\text{m}^3\text{ m}^{-3}$ ), std dev (STD;  $\text{m}^3\text{ m}^{-3}$ ), and CV (std dev normalized by the mean; unitless) for all gauges, gauges that are collocated with in situ soil moisture capacitance probes, and in situ capacitance probes. The temporal statistics are based on the avg from daily spatially averaged soil moisture from the 10 years that in situ soil moisture is available based on daily time series, while the spatial statistics are based on the avg of all daily averaged soil moisture at all gauges.

	Range <sub>sp</sub>	Range <sub>tm</sub>	STD <sub>sp</sub>	STD <sub>tm</sub>	CV <sub>sp</sub>	CV <sub>tm</sub>
All gauge	0.089	0.20	0.020	0.041	0.33	0.64
Collocated gauge	0.072	0.20	0.021	0.041	0.38	0.65
In situ	0.13	0.17	0.037	0.042	0.46	0.48

does not mimic the in situ soil moisture at each individual gauge location, the temporal dynamics are captured very well. The higher spatial variability of observed soil moisture than that of modeled soil moisture in Table 3 is also consistent with previous studies (Brocca et al. 2013; Bertoldi et al. 2014). It is uncertain whether the in situ or all-gauge soil moisture better represents actual spatial variability. However, comparing our model results to Schmugge et al. (1994) during the same time period, the spatial standard deviations are similar, ranging from  $0.0061$  to  $0.056\text{ m}^3\text{ m}^{-3}$ , whereas the prior study found spatial standard deviations ranging from  $0.0026$  to  $0.033\text{ m}^3\text{ m}^{-3}$  using only eight sites. Additionally, we note that the modeled temporal CV is larger than that of the in situ probes, owing to the generally drier modeled soil moisture ( $CV = \sigma/\bar{\theta}$ ; where  $\sigma$  is the standard deviation). However, the modeled spatial CV is lower than that of the in situ probes because the spatial standard deviation of the modeled soil moisture is about half of that of the in situ soil moisture. The collocated gauge results are discussed later in this section. There is also a large interannual variability of seasonally and spatially averaged soil moisture from  $0.05$  to  $0.09\text{ m}^3\text{ m}^{-3}$  in Fig. 7. However, there is no significant temporal trend during the 56-yr period.

During SMEX04, gravimetric soil moisture samples were collected on 11 days at around 1200 local time (LT) at 64 sites within WGEW. Because gravimetric sampling is considered the most accurate measurement, it is useful to compare our results to these samples as an independent test. To directly compare our results with aircraft measurements (discussed below), gravimetric, in situ capacitance probe, and modeled soil moisture are interpolated to  $800\text{-m}$  grids for consistency. Gravimetric samples show much better spatial correlation on average on these 11 days with modeled soil moisture (0.60) than with the capacitance probe data (0.05), partly because only 15 capacitance probes performed properly in that year (Table 2). However, they show a slightly larger

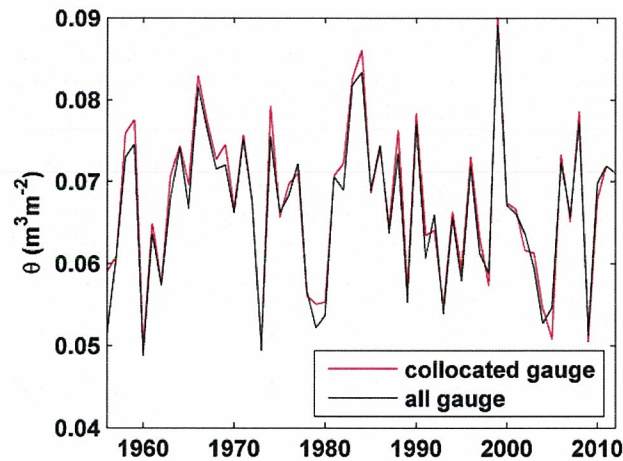


FIG. 7. Seasonally and spatially averaged soil moisture using all gauges collocated with the available in situ capacitance probes (red) and all gauges (black) from 1956 to 2011.

difference in spatial mean from the modeled soil moisture ( $0.03 \text{ m}^3 \text{ m}^{-3}$ ) than from the capacitance probe data ( $0.016 \text{ m}^3 \text{ m}^{-3}$ ). Figure 8 shows the spatial standard deviation of half-hourly soil moisture as a function of spatial mean. In all cases—modeled, capacitance probe, and gravimetric—spatial standard deviation is positively correlated with mean soil moisture. This positive correlation is consistent with the dry soil moisture portion of this curve observed in previous studies (Li and Rodell 2013; Cornelissen et al. 2014).

Precipitation is the driving force of soil moisture in nature and in our water balance model [Eq. (1)]. Therefore, good correlations between precipitation and soil moisture are expected. Indeed, the correlation between seasonally and spatially averaged modeled soil moisture (Fig. 7) and precipitation from 1956 to 2011 is 0.94 (statistically significant at  $<0.001$  level). For each summer, the total precipitation is partitioned into interception, surface runoff, evaporation, drainage, and the change of soil moisture in Eq. (1). On average, these terms account for 7.1%, 9.8%, 24.1%, 59.1%, and  $-0.1\%$  of the total rainfall from 1 July to 30 September from 1956 to 2011. From year to year, these values are also variable. The precipitation that is intercepted ranges from 5.3% to 10.0%, from 2.6% to 18.6% for runoff, from 20.3% to 29.6% for evaporation, and from 54.0% to 64.5% for drainage.

The relationship between daily soil moisture and precipitation can also be explored through their  $e$ -folding time scales (Wang et al. 2006). First, we fit the autocorrelations of daily mean soil moisture and precipitation as exponential functions  $\exp(-t/T)$  of time lag  $t$ . Then, the parameter  $T$  is defined as the  $e$ -folding time scale for each. The time scales of estimated daily mean soil

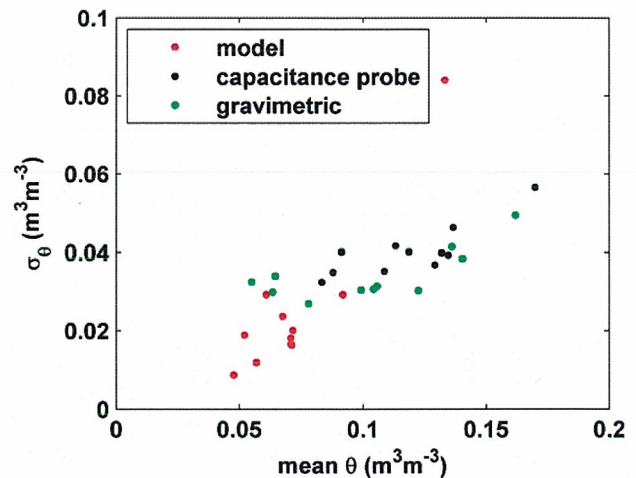


FIG. 8. Spatial std dev of 800-m, 30-min gridded modeled (red), in situ capacitance probe (black), and gravimetric (green) soil moisture as a function of spatially averaged soil moisture for the 11 days during which gravimetric sampling was done during SMEX04.

moisture of the top 7.5 cm in each summer vary from 2.2 to 9.1 days, with an average of 4.6 days, and the 5-cm in situ daily mean soil moisture time scale ranges from 4.3 to 7.1 days, with an average of 5.5 days. These scales are greater than those of daily precipitation (ranging from 1.4 to 2.9 days with an average of 1.8 days), consistent with the finding of Wang et al. (2006). Similarly, we can compute the temporal correlation of daily soil moisture (or precipitation) at two sites separated by distance  $r$  and find that the correlation for soil moisture decreases much slower with  $r$  than that of precipitation. For instance, at  $r = 10$  km, the correlation is still as large as 0.65 for modeled soil moisture, while it is just 0.25 for precipitation. Alternatively, for the same correlation of 0.6, the corresponding  $r$  is 13 km for soil moisture and just 3 km for precipitation. These results are similar for in situ soil moisture and show that daily soil moisture has a longer temporal memory and larger spatial correlation than precipitation.

One obvious benefit of our efforts is the extension of the data period from 10 to 56 years. Another potential benefit is the increased spatial density of data from 19 probes to up to 88 rain gauges. The actual number of gauges recording data ranges from 37 to 88 and varies from year to year. As was noted by Stillman et al. (2013), the variation in number of recording gauges does not tend to affect the spatial statistics associated with daily precipitation. We assume that because soil moisture has higher spatial correlation than precipitation, the effect of varying sample number is insignificant to our results. To evaluate this potential benefit, we compare soil moisture estimates using precipitation from all gauges versus from gauges collocated with soil moisture probes only.

The July–September average soil moisture from all gauges and collocated gauges are nearly identical, with a correlation 0.98 from 1956 to 2011 (Fig. 7), indicating that 13–17 sampling locations are enough to reliably estimate seasonal and areal mean soil moisture over WGEW. However, the spatial range of daily mean soil moisture is affected by the data density. For instance, the average spatial range (highest minus lowest daily gauge-estimated soil moisture on any given day) for all gauges is  $0.11 \text{ m}^3 \text{ m}^{-3}$  in 2010 based on all gauges, versus  $0.087 \text{ m}^3 \text{ m}^{-3}$  using collocated gauges only, and a difference between daily spatial ranges for all gauges and collocated gauges as large as  $0.22 \text{ m}^3 \text{ m}^{-3}$  is observed over the 56 summers. On average, the spatial range is  $0.017 \text{ m}^3 \text{ m}^{-3}$  lower for the collocated gauges than all gauges, as can be noted from Table 3. However, the spatial standard deviation is only slightly affected by the addition of the extra gauges.

One use of the products created in this study is for comparison with other soil moisture products. During SMEX04, soil moisture over WGEW was estimated with two aircraft sensors: the National Aeronautics and Space Administration's (NASA) Two-Dimensional Synthetic Aperture Radiometer (2D-STAR), which uses dual-polarized L-band brightness temperature (Le Vine et al. 2007), and the National Oceanic and Atmospheric Administration's (NOAA) Polarimetric Scanning Radiometer (PSR), which measures microwave brightness temperature (Vivoni et al. 2008), from 5 to 26 August 2004. Additionally, gravimetric soil moisture samples were obtained once daily from 64 locations throughout the watershed on 11 days coinciding with the aircraft overpass time. These, as well as in situ capacitance probe and modeled soil moisture for the corresponding 30-min time step, are interpolated to an 800-m grid for direct comparison with aircraft measurements. On the 3 days with overlapping gravimetric and PSR measurements, the average spatial correlation is small and negative ( $-0.12$ ) and the average difference in spatial means is  $0.036 \text{ m}^3 \text{ m}^{-3}$ . The correlation is much better (0.58) and the average difference is smaller ( $0.0051 \text{ m}^3 \text{ m}^{-3}$ ) on the day with overlapping gravimetric and 2D-STAR measurements. There are capacitance probe and modeled soil moisture estimates for every aircraft overpass, making these more desirable for comparison. Because the gravimetric samples show much better correlation with modeled soil moisture than with capacitance probe measurements, we compare PSR and 2D-STAR with modeled soil moisture. During the four 2D-STAR overpasses, there is an average spatial correlation of 0.42 and average difference of spatial means of  $0.027 \text{ m}^3 \text{ m}^{-3}$ . The correlation of PSR with modeled soil moisture averaged for nine overpasses is near zero (0.014), similar to the

poor correlation between gravimetric and PSR measurements. Further analysis indicates potential problems of the PSR data, such as the nearly uniform measurements of  $0.020 \text{ m}^3 \text{ m}^{-3}$  throughout WGEW from PSR for a few days when the other measurement techniques show significant spatial variability. While the correlation is low, PSR has an average difference of spatial means of only  $0.020 \text{ m}^3 \text{ m}^{-3}$ . It should be noted that the average modeled soil moisture over this time period is  $0.07 \text{ m}^3 \text{ m}^{-3}$ , and therefore, even a relatively small difference of means constitutes a large percentage of the total moisture.

#### 4. Conclusions

The Walnut Gulch Experimental Watershed (WGEW) is subject to highly variable and intermittent summer precipitation from convective thunderstorms associated with the North American monsoon. Soil moisture is continuously monitored by 19 in situ probes at  $\sim 5$ -cm depth across the watershed from 2002 to present. While most of the in situ measurements are reliable, there are several weaknesses of in situ measurements that can often be found in a visual analysis. For example, zero values and very large spikes in the data can be indicative of probe error or surface exposure. The in situ network data quality is analyzed here using various criteria to determine the coverage of "good" measurements. It is found that in any year, 13–17 probes (out of 15–19) with reasonable measurements are available, and that this number of samples spread throughout the watershed is enough to represent the spatially and temporally averaged soil moisture from 1 July to 30 September.

Additionally, a water balance model is calibrated using collocated soil moisture and precipitation measurements to infer soil moisture based solely on rain gauge data. This increases the effective sampling density from the number of reasonable in situ measurements (13–17) to the number of available gauges (37–88; that gathered data in each year) and extends the time period of measurements from 10 (2002–11) to 56 (1956–2011) years. Model accuracy is limited by parameters that are estimated by constants but in reality vary because of site-specific characteristics (i.e., soil type and slope). However, the model is not sensitive to physical conditions that could cause unrealistic measurements in the probes such as water collecting gaps around the sensor and degradation of probe accuracy over time. The model is run assuming minimum soil moisture on 1 June and run for all of June so that on 1 July (day 1 of the study period) the initial conditions are reasonable. After calibration, the daily time series are shown to be highly correlated to observed values at the 19 collocated probes with an average correlation of 0.89.

As an independent evaluation, 64 daily gravimetric samples for 11 days show much better spatial correlation on average with modeled soil moisture (0.60) than with the in situ capacitance probe data (0.05), partly because only 15 capacitance probes performed properly in that year. Both the gravimetric measurements and modeled soil moisture correlate well with the aircraft 2D-STAR measurements but correlate poorly with the aircraft PSR measurements during the SMEX04 because of potential PSR data problems for some of the days. To visualize the spatial distribution of soil moisture, the model-derived soil moisture at each gauge is interpolated to a 100-m grid of WGEW. The daily averaged soil moisture has a spatial range (highest minus lowest 100-m grid box daily soil moisture) as high as  $0.31 \text{ m}^3 \text{ m}^{-3}$  because of localized convection. While no trend persists for the spatially and seasonally averaged soil moisture over this 56-yr time period, large variability from year to year ranging from  $0.05$  to  $0.09 \text{ m}^3 \text{ m}^{-3}$  is found.

Precipitation, the driving force of soil moisture fluctuations, is highly correlated to soil moisture on a seasonal time scale. Daily precipitation and soil moisture are more correlated in a wet year than in a dry year. Daily soil moisture also has a longer temporal memory and larger spatial correlation than precipitation.

Spatially and seasonally averaged soil moisture can be estimated nearly as well with the 13–17 samples collocated with in situ sensors as with samples at all rain gauge locations; however, estimates of daily spatial variability can be significantly hindered using fewer samples. The spatial range of daily soil moisture is as much as  $0.22 \text{ m}^3 \text{ m}^{-3}$  greater using all gauges than using just the collocated sensors. Finally, the 100-m gridded soil moisture products over WGEW for the 56 years can be obtained by contacting the corresponding author.

*Acknowledgments.* All the instruments used in this research are owned and operated by USDA-ARS: the precipitation and soil moisture data used were obtained from the organization's website ([www.tucson.ars.ag.gov/dap/](http://www.tucson.ars.ag.gov/dap/)), and we express our sincere thanks to the staff of the USDA-ARS Southwest Watershed Research Center for their effort and dedication in producing the long-term, high-quality dataset used in this analysis. This research was supported by NSF (Award AGS-0838491 for the COSMOS project; Award EF-1238908 for the macro-systems project).

#### REFERENCES

- Bertoldi, G., S. D. Chiesa, C. Notarnicola, L. Pasolli, G. Niedrist, and U. Tappeiner, 2014: Estimation of soil moisture patterns in mountain grasslands by means of SAR RADARSAT2 images and hydrological modeling. *J. Hydrol.*, **516**, 245–257, doi:10.1016/j.jhydrol.2014.02.018.
- Beven, K. J., and M. J. Kirkby, 1979: A physically based variable contributing area model of basin hydrology. *Hydrol. Sci. Bull.*, **24**, 43–69, doi:10.1080/02626667909491834.
- Brocca, L., T. Tullio, F. Melone, T. Moramarco, and R. Morbidelli, 2012: Catchment scale soil moisture spatial-temporal variability. *J. Hydrol.*, **422–423**, 63–75, doi:10.1016/j.jhydrol.2011.12.039.
- , G. Zucco, T. Moramarco, and R. Morbidelli, 2013: Developing and testing a long-term soil moisture dataset at the catchment scale. *J. Hydrol.*, **490**, 144–151, doi:10.1016/j.jhydrol.2013.03.029.
- Cornelissen, T., B. Diekkrüger, and H. R. Bogen, 2014: Significance of scale and lower boundary condition in the 3D simulation of hydrological processes and soil moisture variability in a forested headwater catchment. *J. Hydrol.*, **516**, 140–153, doi:10.1016/j.jhydrol.2014.01.060.
- Cosh, M. H., T. J. Jackson, S. Moran, and R. Bindlish, 2008: Temporal persistence and stability of surface soil moisture in a semi-arid watershed. *Remote Sens. Environ.*, **112**, 304–313, doi:10.1016/j.rse.2007.07.001.
- Crow, W. T., and Coauthors, 2012: Upscaling sparse ground-based soil moisture observations for the validation of coarse-resolution satellite soil moisture products. *Rev. Geophys.*, **50**, RG2002, doi:10.1029/2011RG000372.
- Dai, Y., and Coauthors, 2003: The Common Land Model. *Bull. Amer. Meteor. Soc.*, **84**, 1013–1023, doi:10.1175/BAMS-84-8-1013.
- Das, N., B. Mohanty, M. H. Cosh, and T. J. Jackson, 2008: Modeling and assimilation of root zone soil moisture using remote sensing observations in Walnut Gulch Watershed during SMEX04. *Remote Sens. Environ.*, **112**, 415–429, doi:10.1016/j.rse.2006.10.027.
- Dickinson, R. E., A. Henderson-Sellers, and P. J. Kennedy, 1993: Biosphere–Atmosphere Transfer Scheme (BATS) version 1e as coupled to the NCAR Community Climate Model. NCAR Tech. Note NCAR-TN-387+STR, 88 pp., doi:10.5065/D67W6959.
- Ek, M. B., K. E. Mitchell, Y. Lin, E. Rogers, P. Grunmann, V. Koren, G. Gayno, and J. D. Tarpley, 2003: Implementation of Noah land surface model advances in the National Centers for Environmental Prediction operational mesoscale Eta model. *J. Geophys. Res.*, **108**, 8851, doi:10.1029/2002JD003296.
- Eltahir, E. A. B., 1998: A soil moisture–rainfall feedback mechanism: 1. Theory and observations. *Water Resour. Res.*, **34**, 765–776, doi:10.1029/97WR03499.
- Entekhabi, D., and Coauthors, 2010: The Soil Moisture Active Passive (SMAP) Mission. *Proc. IEEE*, **98**, 704–716, doi:10.1109/JPROC.2010.2043918.
- Garcia, M., C. D. Peters-Lidard, and D. C. Goodrich, 2008: Spatial interpolation of precipitation in a dense gauge network for monsoon storm events in the southwestern United States. *Water Resour. Res.*, **44**, W05S13, doi:10.1029/2006WR005788.
- Goodrich, D. C., T. O. Keefer, C. L. Unkrich, M. H. Nichols, H. B. Osborn, J. J. Stone, and J. R. Smith, 2008: Long-term precipitation database, Walnut Gulch Experimental Watershed, Arizona, United States. *Water Resour. Res.*, **44**, W05S04, doi:10.1029/2006WR005782.
- Green, W. H., and G. A. Ampt, 1911: Studies on soil physics. *J. Agric. Sci.*, **4**, 1–24, doi:10.1017/S002185960001441.
- Houser, P. R., W. J. Shuttleworth, J. S. Famiglietti, H. V. Gupta, K. H. Syed, and D. C. Goodrich, 1998: Integration of soil moisture remote sensing and hydrologic modeling using data assimilation. *Water Resour. Res.*, **34**, 3405–3420, doi:10.1029/1998WR900001.

Bertoldi, G., S. D. Chiesa, C. Notarnicola, L. Pasolli, G. Niedrist, and U. Tappeiner, 2014: Estimation of soil moisture patterns in mountain grasslands by means of SAR RADARSAT2

- Jackson, T. J., and L. G. McKee, 2009: SMEX04 bulk density and rock fraction data: Arizona. National Snow and Ice Data Center, Boulder, CO, digital media. [Available online at <http://nsidc.org/data/NSIDC-0381>.]
- , D. M. Le Vine, A. Y. Hsu, A. Oldak, P. J. Starks, C. T. Swift, J. D. Isham, and M. I. Haken, 1999: Soil moisture mapping at regional scales using microwave radiometry: The Southern Great Plains hydrology experiment. *IEEE Trans. Geosci. Remote Sens.*, **37**, 2136–2151, doi:10.1109/36.789610.
- Keefer, T. O., M. S. Moran, and G. B. Paige, 2008: Long-term meteorological and soil hydrology database, Walnut Gulch Experimental Watershed, Arizona, United States. *Water Resour. Res.*, **44**, W05S07, doi:10.1029/2006WR005702.
- Kerr, Y. H., P. Waldteufel, J. Wigneron, J. Martinuzzi, J. Font, and M. Berger, 2001: Soil moisture retrieval from space: The soil moisture and ocean salinity (SMOS) mission. *IEEE Trans. Geosci. Remote Sens.*, **39**, 1729–1735, doi:10.1109/36.942551.
- Koster, R. D., and M. J. Suarez, 2001: Soil moisture memory in climate models. *J. Hydrometeor.*, **2**, 558–570, doi:10.1175/1525-7541(2001)002<0558:SMMICM>2.0.CO;2.
- Kustas, W. P., and D. C. Goodrich, 1994: Preface [to special section on Monsoon '90 Multidisciplinary Experiment]. *Water Resour. Res.*, **30**, 1211–1225, doi:10.1029/93WR03068.
- Le Vine, D. M., T. J. Jackson, and M. Haken, 2007: Initial images of the synthetic aperture radiometer 2D-STAR. *IEEE Trans. Geosci. Remote Sens.*, **45**, 3623–3632, doi:10.1109/TGRS.2007.903830.
- Li, B., and M. Rodell, 2013: Spatial variability and its scale dependency of observed and modeled soil moisture over different climate regions. *Hydrol. Earth Syst. Sci.*, **17**, 1177–1188, doi:10.5194/hess-17-1177-2013.
- Orth, R., R. D. Koster, and S. I. Seneviratne, 2013: Inferring soil moisture memory from streamflow observations using a simple water balance model. *J. Hydrometeor.*, **14**, 1773–1790, doi:10.1175/JHM-D-12-099.1.
- Osterkamp, W. R., 2008: Geology, soils, and geomorphology of the Walnut Gulch Experimental Watershed, Tombstone, Arizona. *J. Ariz.-Nev. Acad. Sci.*, **40**, 136–154, doi:10.2181/1533-6085-40.2.136.
- Pan, F., 2012: Estimating daily surface soil moisture using a daily diagnostic soil moisture equation. *J. Irrig. Drain. Eng.*, **138**, 625–631, doi:10.1061/(ASCE)IR.1943-4774.0000450.
- , C. D. Peters-Lidard, and M. J. Sale, 2003: An analytical method for predicting surface soil moisture from rainfall observations. *Water Resour. Res.*, **39**, 1314, doi:10.1029/2003WR002142.
- Pellarin, T., S. Louvet, C. Gruhier, G. Quantin, and C. Legout, 2013: A simple and effective method for correcting soil moisture and precipitation estimates using AMSR-E measurements. *Remote Sens. Environ.*, **136**, 28–36, doi:10.1016/j.rse.2013.04.011.
- Peters-Lidard, C. D., D. M. Mocko, M. Garcia, J. A. Santanello Jr., M. A. Tischler, M. S. Moran, and Y. Wu, 2008: Role of precipitation uncertainty in the estimation of hydrologic soil properties using remotely sensed soil moisture in a semiarid environment. *Water Resour. Res.*, **44**, W05S18, doi:10.1029/2007WR005884.
- Rim, C.-S., and L. W. Gay, 2002: Estimating soil moisture in small watersheds, using a water balance approach. *Nord. Hydrol.*, **33**, 373–390.
- Robinson, D. A., and Coauthors, 2008: Soil moisture measurement for ecological and hydrological watershed-scale observatories: A review. *Vadose Zone J.*, **7**, 358–389, doi:10.2136/vzj2007.0143.
- Ryu, D., T. J. Jackson, and R. Bindlish, 2010: Soil moisture retrieval using a two-dimensional L-band synthetic aperture radiometer in a semiarid environment. *IEEE Trans. Geosci. Remote Sens.*, **48**, 4273–4284, doi:10.1109/TGRS.2010.2051677.
- Seneviratne, S. I., and Coauthors, 2006: Soil moisture memory in AGCM simulations: Analysis of Global Land–Atmosphere Coupling Experiment (GLACE) data. *J. Hydrometeor.*, **7**, 1090–1112, doi:10.1175/JHMS33.1.
- Schmugge, T., T. J. Jackson, W. P. Kustas, R. Roberts, R. Parry, D. C. Goodrich, S. A. Amer, and M. A. Weltz, 1994: Push broom microwave radiometer observations of surface soil moisture in Monsoon '90. *Water Resour. Res.*, **30**, 1321–1327, doi:10.1029/93WR03057.
- Small, E. E., 2001: The influence of soil moisture anomalies on variability of the North American Monsoon System. *Geophys. Res. Lett.*, **28**, 139–142, doi:10.1029/2000GL011652.
- Stillman, S., X. Zeng, W. J. Shuttleworth, D. C. Goodrich, C. L. Unkrich, and M. Zreda, 2013: Spatiotemporal variability of summer precipitation in southeastern Arizona. *J. Hydrometeor.*, **14**, 1944–1951, doi:10.1175/JHM-D-13-017.1.
- USDA, 2007: Southwest Watershed Research Center and Walnut Gulch Experimental Watershed. USDA Doc., 40 pp. [Available online at [www.ars.usda.gov/SP2UserFiles/Place/53424500/SWRCWGEW\\_2007.pdf](http://www.ars.usda.gov/SP2UserFiles/Place/53424500/SWRCWGEW_2007.pdf).]
- Van Genuchten, M. Th., 1980: A closed-form equation for predicting the hydraulic conductivity of unsaturated soils. *Soil Sci. Soc. Amer. J.*, **44**, 892–898, doi:10.2136/sssaj1980.03615995004400050002x.
- Vereecken, H., J. A. Huisman, H. Bogaen, J. Vanderborght, J. A. Vrugt, and J. W. Hopmans, 2008: On the value of soil moisture measurements in vadose zone hydrology: A review. *Water Resour. Res.*, **44**, W00D06, doi:10.1029/2008WR006829.
- Verhoef, A., J. Fernandez-Galvez, A. Diaz-Espejo, B. E. Main, and M. El-Bishti, 2006: The diurnal course of soil moisture as measured by various dielectric sensors: Effects of soil temperature and the implications for evaporation estimates. *J. Hydrol.*, **321**, 147–162, doi:10.1016/j.jhydrol.2005.07.039.
- Vivoni, E. R., M. Gebremichael, C. J. Watts, R. Bindlish, and T. J. Jackson, 2008: Comparison of ground-based and remotely sensed soil moisture estimates over complex terrain during SMEX04. *Remote Sens. Environ.*, **112**, 314–325, doi:10.1016/j.rse.2006.10.028.
- Wang, A. H., X. Zeng, S. S. P. Shen, Q.-C. Zeng, and R. E. Dickinson, 2006: Timescales of land surface hydrology. *J. Hydrometeor.*, **7**, 868–879, doi:10.1175/JHM527.1.
- Xia, Y., and Coauthors, 2012: Continental-scale water and energy flux analysis and validation for the North American Land Data Assimilation System project phase 2 (NLDAS-2): 1. Inter-comparison and application of model products. *J. Geophys. Res.*, **117**, D03109, doi:10.1029/2011JD016048.
- Zreda, M., W. J. Shuttleworth, X. Zeng, C. Zweck, D. Desilets, T. Franz, and R. Rosolem, 2012: COSMOS: The Cosmic-ray Soil Moisture Observing System. *Hydrol. Earth Syst. Sci.*, **16**, 4079–4099, doi:10.5194/hess-16-4079-2012.

Copyright of Journal of Hydrometeorology is the property of American Meteorological Society and its content may not be copied or emailed to multiple sites or posted to a listserv without the copyright holder's express written permission. However, users may print, download, or email articles for individual use.

---